

# Final Progress Report

Program: NASA NRA-97-MTPE-16  
PIs David S. Covert and Theodore L. Anderson  
University of Washington, Seattle, WA  
Title Validation of the lidar retrieval of aerosol extinction  
Period June, 1999 - May 2002

## Part I: Overview

### *Summary:*

The goal of this project is to facilitate the integration of Light Detection and Ranging (lidar) measurements in building a global aerosol climatology. Lidar is sensitive to aerosol even at modest concentrations, provides vertical resolution, and is capable of surveying large regions of the troposphere - indeed, upcoming satellite missions will provide truly global surveys. However, quantitative interpretation of lidar data requires knowledge of the extinction-to-backscatter ratio,  $S_a$ . As such, the focus of our project has been to develop a database and an approach to constraining  $S_a$ . As shown below, knowledge of  $S_a$  for tropospheric aerosols was highly unconstrained at the outset of this project and is much better constrained today (due to the efforts of several groups, not just our own). Two case studies using spaceborne lidar data are used below to demonstrate the vast reduction of uncertainty in lidar retrievals that is associated with moving from unconstrained  $S_a$  to constrained  $S_a$ .

Prior to this project, our group developed a method for calibrated, in situ measurement of  $S_a$  (Doherty et al., 1999, Appl. Optics, 38, 1823). During the course of this project, we deployed this technology in several field campaigns to obtain characteristic values for a wide range of aerosol types and to study the physical/chemical/thermodynamic parameters that control variations in  $S_a$ . This grant was the primary source of support for one field campaign (LINC) and for the analysis of  $S_a$  from all field campaigns.

While considerable progress has been made over the three years of this project, a great deal remains to be done. As documented below, the recent increase in data on  $S_a$  has been extraordinary. These data come from our approach as well as approaches based on Raman lidar, slant-path lidar, and sunphotometry. The challenge ahead is to integrate these data and to develop and test methods of constraining  $S_a$  throughout the global troposphere. The planned launch in 2004 of the ESSP3-CENA satellite (a lidar satellite to fly in formation with the many aerosol sensors on NASA's Aqua satellite) provides a compelling target date for achieving this larger goal. As described herein, our research has helped to lay the foundation for this larger project, which will form the basis of a subsequent proposal.

### *Yearly breakdown of activities*

year 1: June 1999 - May 2000	INDOEX, LINC*, and SEAS field campaigns
year 2: June 2000 - May 2001	ACE-Asia field campaign
year 3: June 2001 - May 2002	analysis, publication

\*LINC campaign was primarily funded through this grant.

## Part II: Publications

### *Primary publications for GACP bibliography:*

Anderson, T. (1999) Chapter 5: Extinction-to-backscatter ratio database in PICASSO-CENA: Lidar Algorithm Theoretical Basis Document White Papers, NASA Langley, Oct. 8, 1999. 55-63.

URL: <http://www.atmos.washington.edu/~cheeka/PC/whitepapers.html>

Anderson, T. L., Masonis, S. J., Covert, D. S., Charlson, R. J. and Rood, M. J., (2000): In-situ measurement of the aerosol extinction-to-backscatter ratio at a polluted, continental site, *J. Geophys. Res.*, 105, 26907-26915.

URL: <http://www.atmos.washington.edu/~cheeka/linc/SaLINCjgr.html>

Masonis, S. J., Franke, K., Ansmann, A., Mueller, D., Althausen, D., Ogren, J. A., Jefferson, A. and Sheridan, P. J., (2001): An intercomparison of aerosol light extinction and 180° backscatter as derived using in-situ instruments and Raman lidar during the INDOEX field campaign, *J. Geophys. Res.*, in press.

URL: not yet available

Stephens, G. L., Vaughan, M., Engelen, R. J. and Anderson, T. L., (2001): Toward retrieving properties of the tenuous atmosphere using space-based Lidar measurements, *J. Geophys. Res.*, in press.

URL: not yet available

### *Additional publications partially supported by this project:*

Anderson, T. L., Covert, D. S. and Ghan, S. J., (2001): A practical index of aerosol type for transport modeling, satellite retrievals, and in-situ measurements, manuscript in preparation.

URL: <http://www.atmos.washington.edu/~cheeka/Rmass/Rmass.html>

Anderson, T., Eisele, F., Schmidt, U., Tyndall, G. and Winker, D. (2001) Chapter 5: Instrumentation in Atmospheric Chemistry in a Changing World, G. Brasseur (Eds.)

URL: not yet available

Rodhe, H., Charlson, R. J. and Anderson, T. L., (2000): Avoiding circular logic in climate modeling, *Climatic Change*, 44, 419-422.

URL: none

## Part III: Detailed report

This section describes progress made toward an empirically based constraint on the aerosol extinction-to-backscatter ratio,  $S_a$ , for application to simple, elastic-scatter lidar systems, especially spaceborne lidar.

### Definitions

*Lidar equation:* An elastic backscatter lidar responds to a convolution of local  $180^\circ$  backscattering,  $\beta$ , and path-integrated extinction,  $\sigma$ :

$$P(r) = \frac{C\beta(r)}{r^2} \exp\left[-2\int_0^r \sigma(r') dr'\right] \quad (1)$$

where  $r$  is the range,  $P(r)$  is the detected power, and  $C$  is the instrument calibration constant.

*Aerosol extinction-to-backscatter ratio,  $S_a$ :* The deconvolution of  $\beta$  and  $\sigma$  can be accomplished given independent knowledge of the extinction-to-backscatter ratio,  $S$ . Since the optical properties of air are well known, the problem reduces to understanding the *aerosol* extinction-to-backscatter ratio,  $S_a$ :

$$S_a = \frac{\sigma_e}{\beta} = \frac{\sigma_s + \sigma_a}{\beta} \quad (2)$$

where  $\sigma_e$  is the extinction coefficient due to aerosol particles and  $\sigma_s$ , and  $\sigma_a$  are the components of aerosol extinction due to scattering and absorption, respectively.

### Importance of $S_a$ for quantitative backscatter and extinction retrievals

Sensitivity analysis has been performed using spaceborne lidar data from the LITE shuttle mission (Winker et al., 1996) under two alternate assumptions:

Unconstrained  $S_a$   
factor of 4 uncertainty (20-80 sr)

Constrained  $S_a$   
factor of 1.5 uncertainty (either 20-30 sr or 40-60 sr)

Results (shown graphically in Figures 1 and 2) can be summarized as follows:

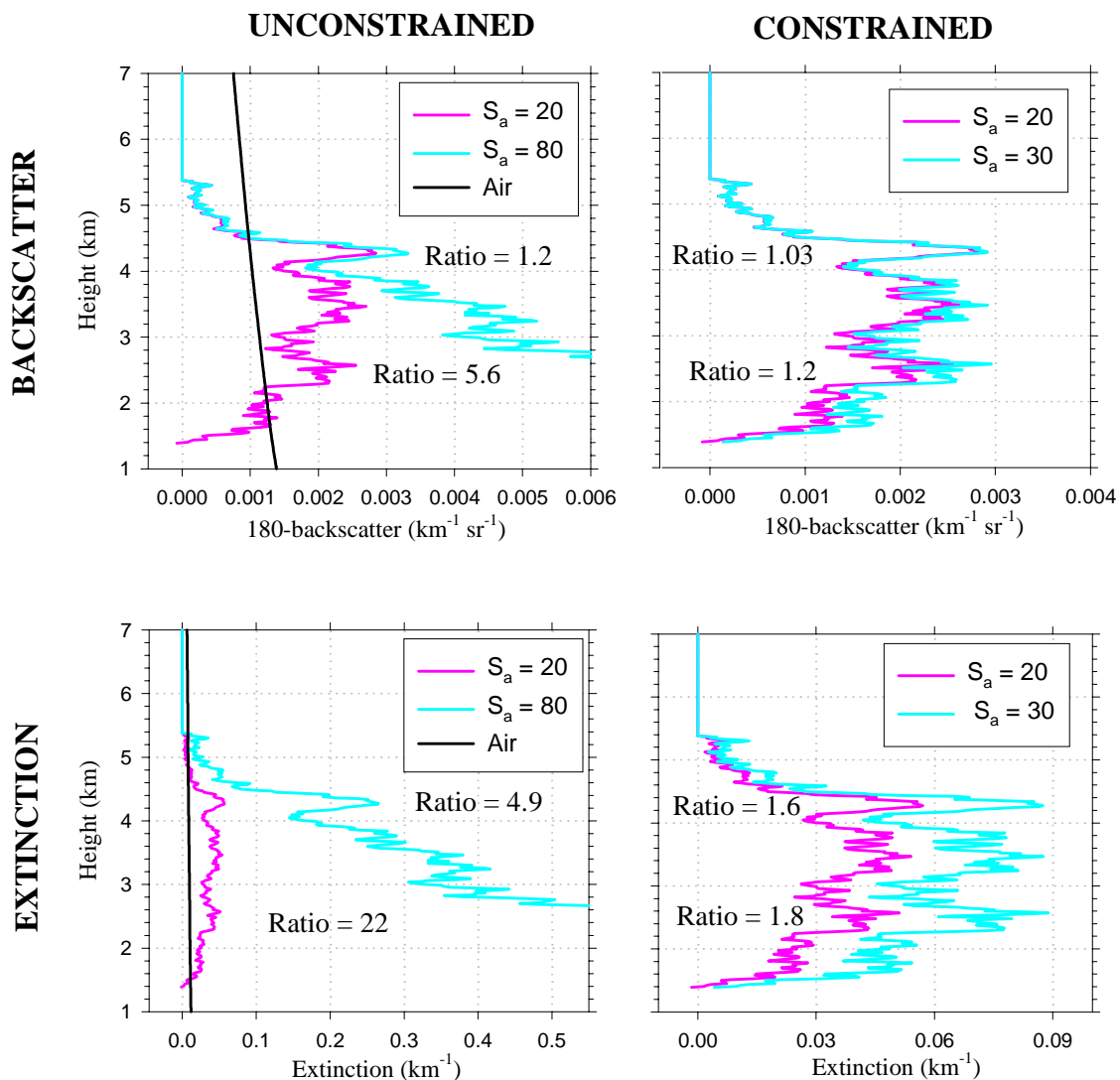
With **unconstrained  $S_a$**  you (only) get:

- accurate backscatter at top of first layer

With **constrained  $S_a$**  you get:

- accurate backscatter profiles
- considerable bounding of extinction profiles

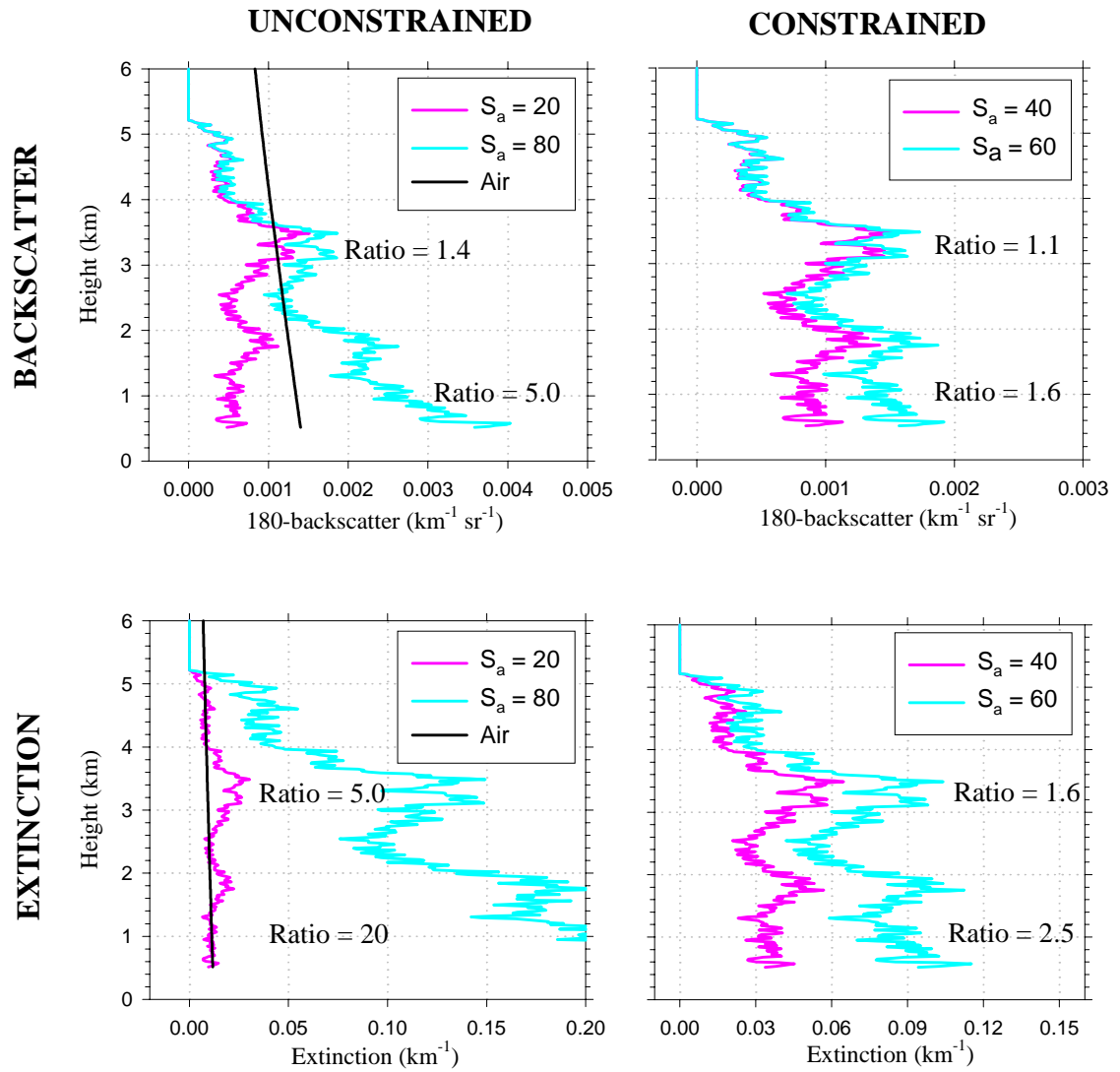
LITE, Orbit 147, lofted Sahara dust layer over Atlantic



data from Mark Vaughan, plot by Tad Anderson, July 1, 2001

**Figure 1:** Retrieved profiles of aerosol backscatter and extinction from spaceborne lidar acquired during the Lidar In-Space Technology (LITE) experiment, Sept., 1994. The "Ratio" values shown on the plots are the ratios of unconstrained to constrained values at the indicated location of the profile. The case shown applies to a Saharan dust layer over the Atlantic Ocean.

LITE, Orbit 129, boundary layer aerosol under thin cirrus



data from Mark Vaughan, plot by Tad Anderson, July 1, 2001

Figure 2: As in Fig. 1 except for a boundary layer aerosol beneath thin cirrus.

## Empirical knowledge of $S_a$

Given its importance to lidar retrievals, we undertook the task of assessing the state of knowledge of  $S_a$  for tropospheric aerosols. Our initial literature review, in 1999, showed an overall paucity of measurements, but did permit three useful insights:

1. geographical location by itself does not constrain  $S_a$
2. the measured range is about 10 to 100 sr
3. coarse-mode aerosol is generally toward low end of range;  
pollution aerosol is generally toward high end of range

The literature review is summarized in Table 1, below, adapted from Anderson et al. (2000).

Table 1: Measurements of  $S_a$  for tropospheric aerosols, as of 1999

<i>Method</i>	<i>Location</i>	$N^{(a)}$	$S$ (sr)
slant-path lidar (b)	mixed layer, west U.S. (Tucson, AZ)	57	15-82
horizontal lidar (c)	Netherlands	10	10-50
horizontal lidar (d)	marine surface layer, Australian coast	10	40-80
multi-wave lidar (e)	marine boundary layer (tropical Atlantic)	1	<30
	mixed layer over rainforest (S. Amer.)	1	43-60
	Saharan dust aloft (tropical Atlantic)	2	15-62
backscatter-sonde (f)	rural, arid SW U.S.	12	42
	rural western U.S. lower troposphere	4	15-30
	rural western U.S. upper troposphere	4	15-60
space-borne lidar (g)	smoke layers in SH upper troposphere	7	50-90
Raman lidar (h)	polluted boundary layer over Leipzig, Germany	1	55-95

<sup>a</sup> Approximate number of independent samples.

<sup>b</sup> Determines effective  $S$  over mixed layer at 694 nm. (Spinhirne et al., 1980; Reagan et al., 1984; 1988)

<sup>c</sup> 1064 nm laser. No information on location of instrument or type of aerosol investigated. (de Leeuw et al., 1986)

<sup>d</sup> 532 nm laser beam aimed 2 m over ocean surface from coastal site. Effect of waves not assessed. (Young et al., 1993).

<sup>e</sup>  $S$  at 600 nm is constrained by Mie calculations based on the measured wavelength variation of  $\beta_p$ . (Sasano and Browell, 1989)

<sup>f</sup>  $S$  reported at 690 nm. Method requires significant wavelength and angular adjustments, based on assumed size distributions and Mie calculations. (Rosen et al., 1997a, b)

<sup>g</sup>  $S$  at 532 nm is constrained to values yielding physically plausible lidar retrievals under the assumption of constant  $S$  throughout upper troposphere. (Kent et al., 1998)

<sup>h</sup>  $S$  at 532 nm determined from independent extinction measurements using nitrogen-Raman. (Ansmann et al., 1992; Muller et al., 1998)

But it is not enough to have individual measurements of  $S_a$  that are not coupled to other aerosol and atmospheric properties. In order to (i) determine the variability of  $S_a$ , and (ii) establish parameterizations of  $S_a$  and (iii) understand the accuracy of these parameterizations, we need:

- sufficiently large data sets for statistical analysis
- simultaneous, collocated measurements of thermodynamic state
- simultaneous, collocated measurements of aerosol composition
- vertical resolution sufficient to distinguish major aerosol layers

Viewed in this light, the situation just two years ago with regard to empirical measurements of  $S_a$  looked bleak, as shown in Table 2a:

Table 2a:  $S_a$  measurements with significant sample sizes before **1999**

<i>method</i>	<i>location</i>	<i>notes</i>	$S_a$ <i>range</i>	<i>sample size</i>	<i>thermo-dynam. state?</i>	<i>aerosol composition?</i>	<i>vertical resol.?</i>
slant lidar	Tucson, AZ	a	15 - 82	57	yes	no	no

"N": estimated number of independent samples

" $S_a$  range": range that encompasses 95% of the data

(a) Lidar measurements at several slant angles determines effective  $S$  over mixed layer at 694 nm; sporadic daily samples over 3 years [Reagan et al., 1988].

However, spurred by the prospect of global lidar data from satellites, the community has made great strides in developing adequate data sets. Table 2b, below, shows data sets currently published or in press. Keep in mind that several other data sets (e.g. from PRIDE, SAFARI, ACE-Asia, AERONET) are in the works. This Table reflects analysis by our group and is adapted from a co-authored paper (Stephens et al., 2001).

Table 2b:  $S_a$  measurements with significant sample sizes

<i>method</i>	<i>location</i>	<i>notes</i>	$S_a$ <i>range</i>	<i>sample size</i>	<i>thermo-dynam. state?</i>	<i>aerosol composition?</i>	<i>vertical resol.?</i>
slant lidar	Tucson, AZ	a	15 - 82	57	yes	no	no
nephelometry	central Illinois	b	27 - 75	95	yes	yes	no
nephelometry	Indian Ocean	c	33 - 91	168	yes	yes	yes
nephelometry	Hawaiian coast	d	26 - 33	35	yes	yes	no
lidar/sunpho.	Indian Ocean	e	25 - 75	102	yes	surface	no
Raman lidar	Oklahoma	f	45 - 87	2556	yes	no	yes
nephelometer	Asian outflow	g	35 - 65	~200	yes	yes	yes

"N": estimated number of independent samples

" $S_a$  range": range that encompasses 95% of the data

- (a) Lidar measurements at several slant angles determines effective  $S$  over mixed layer at 694 nm; sporadic daily samples over 3 years [Reagan et al., 1988].
- (b) Nephelometric method determines local  $S$  at 532 nm; continuous surface measurements over 5 weeks; N assumes 1 independent sample every 4 hours [Anderson et al., 2000].
- (c) Method as in (b); airborne data (30 to 3500 m altitude) from 18 flights over 6 weeks during low-level offshore flow from surrounding continents; N assumes 1 independent sample every 1 km vertical or 100 km horizontal [Masonis, 2001; Masonis et al., 2001].
- (d) Method as in (b); continuous surface measurements over 8 days during onshore (marine) flow; N assumes 1 independent sample every 4 hours [Masonis, 2001].
- (e) Vertically pointing Micro Pulse Lidar and sunphotometer determine effective  $S$  over aerosol-laden lower troposphere; continuous data from ship during same experiment as in (c); N assumes one independent sample every 4 hours for the 17 cloud-free days of data [Welton et al., 2001].
- (f) Raman lidar determines local  $S$  from 0.8 km to about 4 km at 355 nm; continuous data from surface station over 2 years; N assumes 4 independent samples in vertical obtained every 4 hours over 213 days with 50% data loss due to cloud contamination [Ferrare et al., 2001].
- (g) Method as in (b); airborne data (30 to 6000 m altitude) from 19 flights over 6 weeks primarily in the Yellow Sea and Sea of Japan during the ACE-Asia campaign, Spring, 2000; N assumes 1 independent sample every 1 km vertical or 100 km horizontal [Anderson, TL, Masonis, SJ, unpublished data].



Two of these data sets reveal remarkable consistencies in the cases of clean marine seasalt (Figure 3) and sulfate-dominated pollution from the midwestern US (Figure 4).

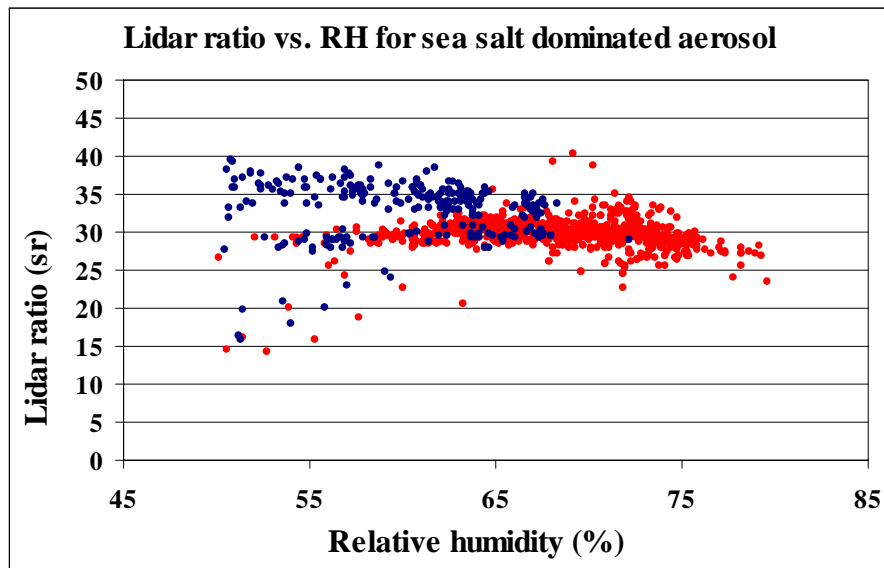


**Figure 3:** Lidar ratio versus the relative humidity at which it was measured during the SEAS field campaign, Bellows Fields, Oahu, Hawaii (March-April, 2000; Masonis, 2001, PhD dissertation, University of Washington). For most of the campaign the aerosol was characterized as clean marine (red), but some of the samples were influence by volcanic aerosol from Japan (blue).

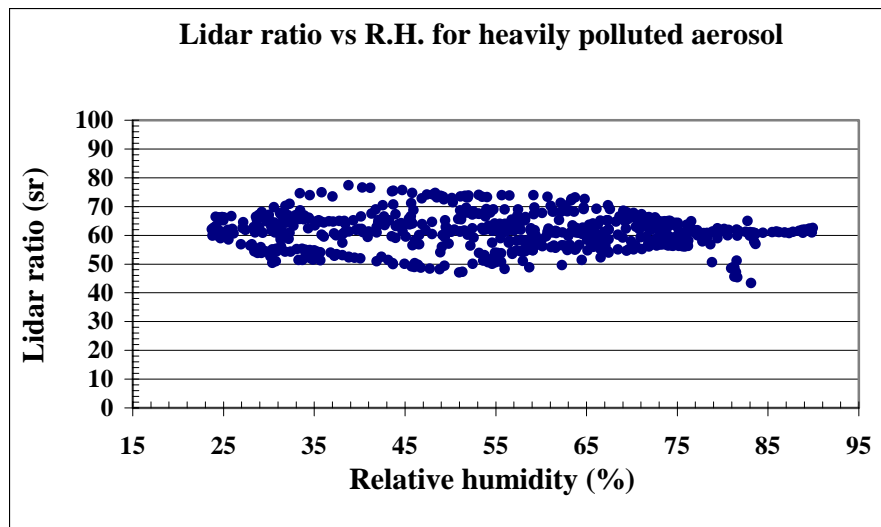


**Figure 4:** Lidar ratio versus the relative humidity at which it was measured. Nephelometric technique [Doherty et al., 1999, Appl. Optics, 38, 1823-1832.] These data were collected during the LINC field campaign in Bondville, Illinois (August-September, 1999; Anderson et al., 2000, J. Geophys. Res., 105, 26907-26915) during times when the aerosol was characterized as heavily polluted.

In other cases, the data reveal useful relationships for building parameterizations. For example, Fig. 5 shows a strong relation between  $S_a$  and the fraction of aerosol volume in fine mode.

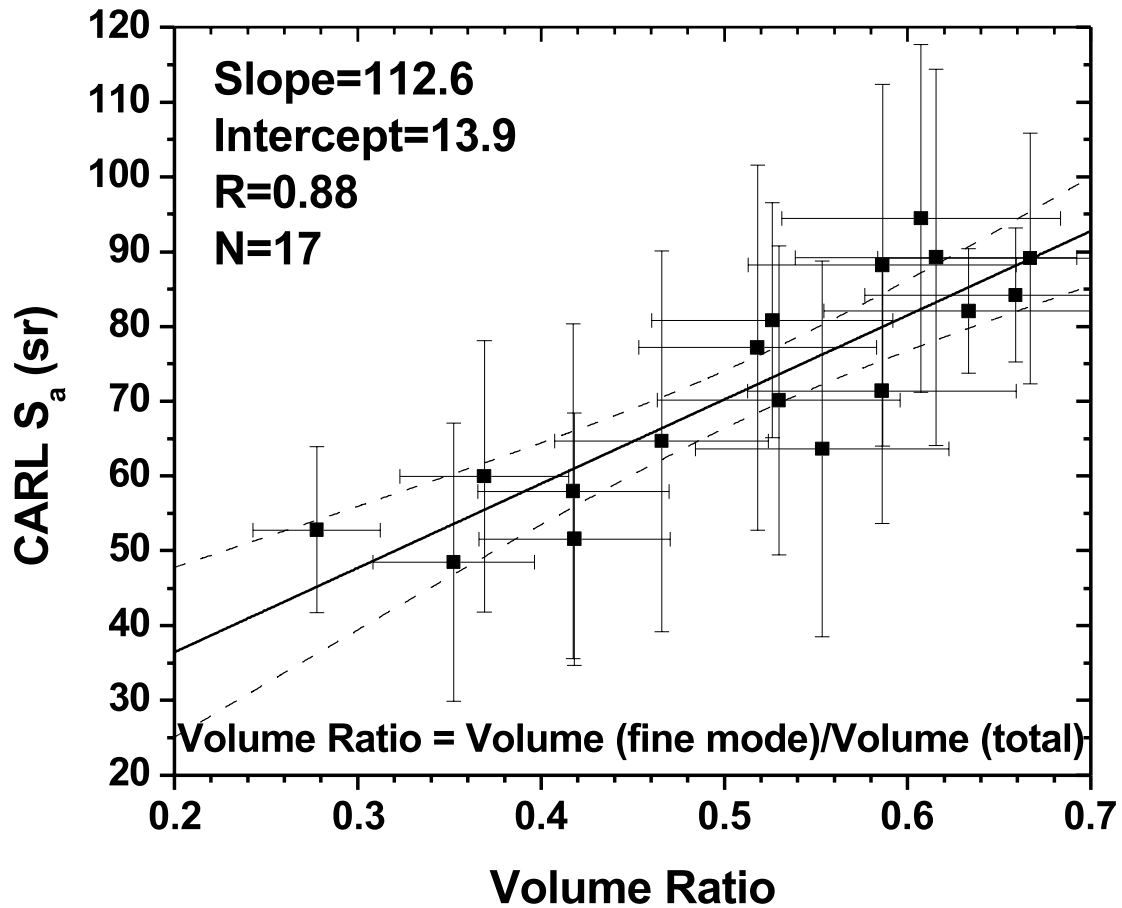
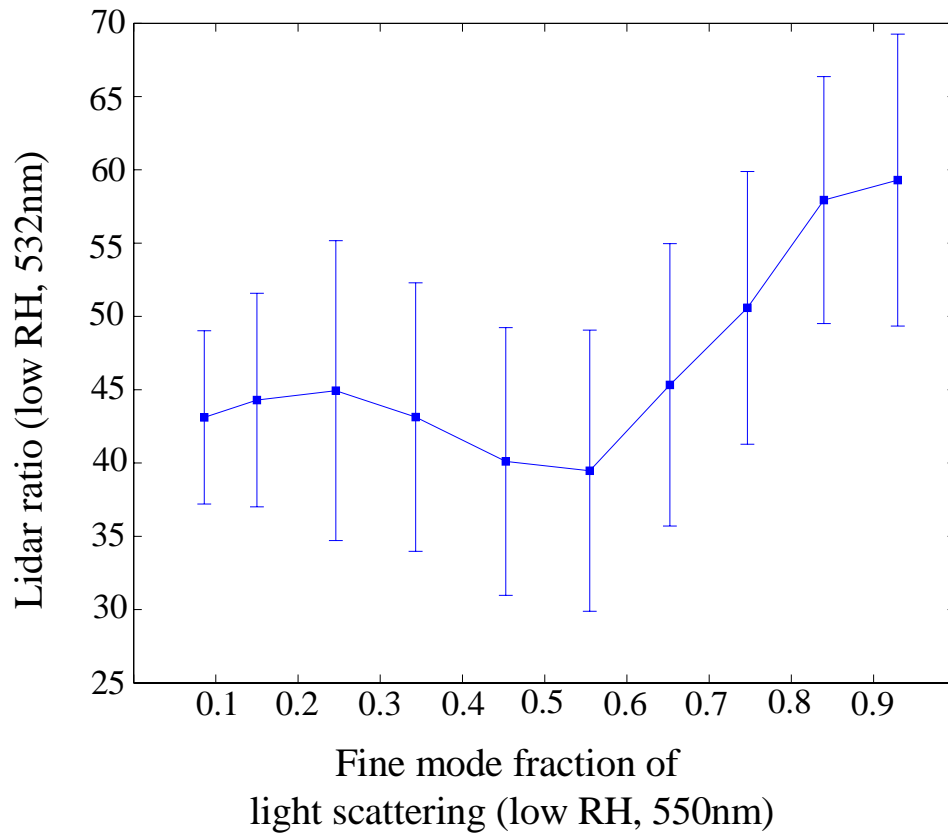


Figure 5: Aerosol extinction-to-backscatter ratio,  $S_a$ , at 355 nm wavelength measured by Raman lidar versus the fine-mode fraction of aerosol volume derived by inversion of sunphotometer/radiometer measurements. All measurements at DOE Southern Great Plains site in central Oklahoma. Cases chosen for comparison had aerosol optical depth (at 440 nm) greater than 0.2 and vertical variation in  $S_a$  less than 10 sr. [Ferrare et al., 2001, J. Geophys. Res., in press]

Similarly, Fig. 6 shows a relationship between  $S_a$  and the fraction of aerosol scattering in fine mode.



**Figure 6:** Airborne, nephelometric measurements of  $S_a$  versus the fine-mode fraction of aerosol light scattering,  $\sigma_{sp}$ . Data from 19 flights over the Yellow Sea and Sea of Japan during the Asian dust season, ACE-Asia. Means and standard deviations are shown. Curiously, the expected relationship was found only for fine-mode fractions of 50% or more. [Anderson, TL and Masonis, SJ, unpublished data]

Figures 7 and 8 show relationships, from two different campaigns, between  $S_a$  and height. For pollution aerosol advected over the Indian Ocean (INDOEX campaign), variation in the vertical has been shown to have a consistent structure (Fig. 7). For dust and pollution aerosol advected over the Yellow Sea and Sea of Japan (ACE-Asia), no systematic variation in the vertical was observed (Fig. 8).

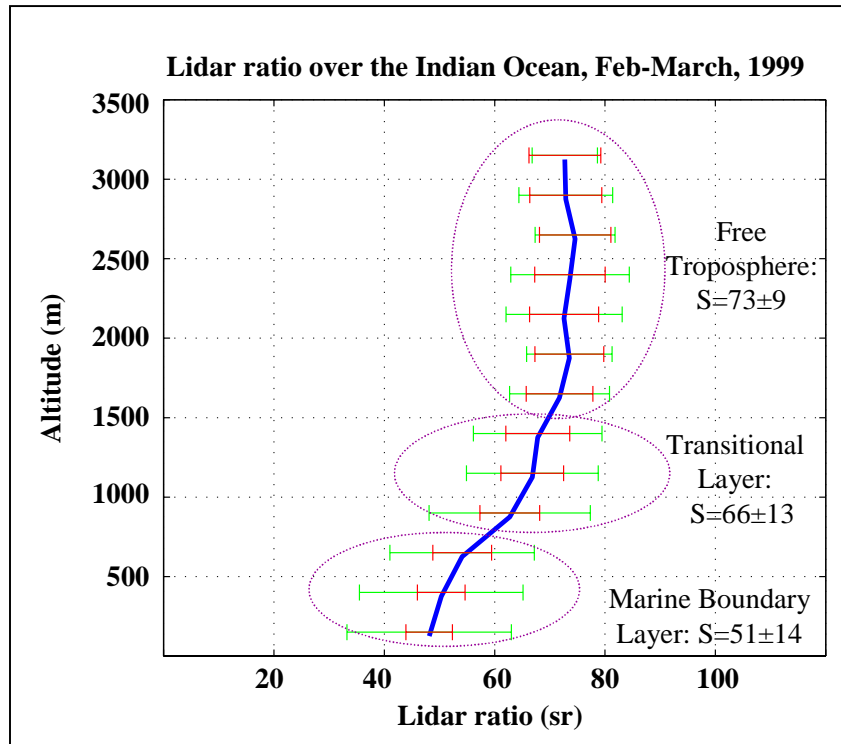


Figure 7: Lidar ratio versus altitude over the Indian Ocean during the northeast monsoon (blue), as measured during INDOEX. The standard deviation at each altitude is shown in green, and the uncertainty of the mean (95% C.I.) in red.

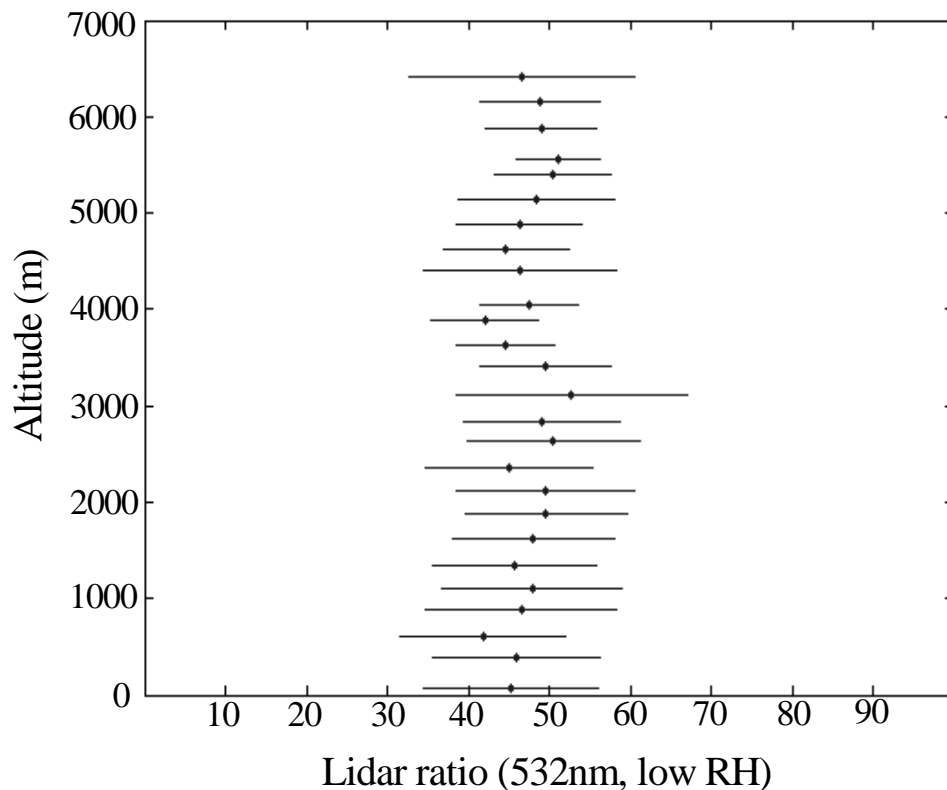


Figure 8: Airborne, nephelometric measurements of  $S_a$  from 19 flights over the Yellow Sea and Sea of Japan during the Asian dust season, ACE-Asia. Means and standard deviations are shown for data grouped by altitude. [Anderson, TL and Masonis, SJ, unpublished data]

## Dust enigma

There is conflicting evidence concerning the appropriate value of  $S_a$  for mineral dust aerosol. This section outlines the evidence on both sides.

### Evidence that dust- $S_a$ is low (20-30 sr at 532 nm):

#### 1. "theory":

20 +/- 5 sr

OPAC "mineral aerosol model" combined with Mie calculations [Ackermann, 1998].

However, calculation assumes spheres.

#### 2. Tucson measurements:

~25 sr

Extensive slant-path lidar measurements by Reagan et al. [1988] at 694 nm show a dominant cluster at  $S_a = \sim 25$  sr. However, *some* measurements, even with measured mass dominated by coarse mode, do show values around 40 sr.

### 3. LITE measurements:

25 - 35 sr

Lofted aerosol layers were observed by LITE over Atlantic during a large Saharan dust outflow event. Retrieval of optical depth and  $S_a$  by transmission method indicated  $S_a = 25 - 35$  sr at 532 nm [Karyampudi et al., 1999]. However, estimate uses a correction for multiple scattering which is based on an assumed scattering phase function.

### ***Evidence that dust- $S_a$ is high (35-50 sr at 532 nm):***

#### 1. Non-spherical theory:

$S_a$  should be higher

For coarse-mode, non-spherical particles, spherical (Mie) calculations significantly overestimate  $180^\circ$  backscattering but have little effect on total scattering [Mishchenko et al., 1995] such that they underestimate extinction-to-backscatter. However, these non-spherical predictions for  $180^\circ$  backscattering have not been confirmed experimentally.

#### 2. Sahara dust measurements in ACE-2:

~ 36 sr

Welton et al. [2000]

37 +/- 9 sr

Powell et al. [2000]

35 +/- 5 sr

However, this is only one dust event, and it is not known how much non-dust (e.g. pollution) aerosol was mixed with the dust.

#### 3. Dust measurements in ACE-Asia:

43 +/- 6 sr

Nephelometric technique; data from flights/dust events; dust cases identified when coarse-mode fraction of scattering is  $> 80\%$  [Anderson and Masonis, unpublished data.] However, results are preliminary and unpublished.

### ***Further caveats:***

1. These discrepancies could reflect real atmospheric variability. It is possible that dust- $S_a$  is not a constant, but varies as a function of:

- source region (via changes in mineral composition)
- distance from source (via changes in size-distribution)

2. Measurements and analysis aimed at resolving this discrepancy (e.g. via method comparisons) are underway.

## **Conclusions and Implications**

- Profiles of aerosol backscatter and extinction from elastic backscatter lidar (e.g. as will be deployed from space in upcoming NASA missions) can be retrieved with greater accuracy if  $S_a$  can be constrained. Sensitivity studies indicate that knowing  $S_a$  to within about a factor of 1.5 is required for meaningful, quantitative retrievals.
- Geographical location does not, by itself, provide an adequate constraint.
- Empirical knowledge of  $S_a$  has grown tremendously in the past 2 years. These data reveal many circumstances where  $S_a$  is either invariant or varies in a predictable way.
- The appropriate value(s) of  $S_a$  for mineral dust is uncertain and is an area of active research.
- Creating a global look-up table of  $S_a$  for use by satellite lidar appears to be feasible.
- To make optimal use of the growing empirical database, the look-up table must include all of the following elements:
  - geographical location, vertical location, season
  - major aerosol types expected in that time/location
  - criteria for deciding which of the expected aerosol types is present. These criteria should not require knowledge of  $S_a$ . Likely candidates would be top-of-layer backscatter magnitude for detecting plumes and the backscatter color ratio as an indicator of coarse-mode fraction.

## **Bibliography**

- Ackermann, J., (1998): The extinction-to-backscatter ratio of tropospheric aerosol: A numerical study, *J. Atmos. Ocean. Technol.*, **15**, 1043-1050.
- Anderson, T. L., Covert, D. S., Wheeler, J. D., Harris, J. M., Perry, K. D., Trost, B. E. and Jaffe, D. J., (1999): Aerosol backscatter fraction and single scattering albedo: measured values and uncertainties at a coastal station in the Pacific NW, *J. Geophys. Res.*, **104**, 26793-26807.
- Anderson, T. L. and Ogren, J. A., (1998): Determining aerosol radiative properties using the TSI 3563 integrating nephelometer, *Aerosol Sci. Technol.*, **29**, 57-69.
- Ansmann, A., Riebesell, M., Wandinger, U., Weitkamp, C., Voss, E., Lahmann, W. and Michaelis, W., (1992): Combined Raman elastic-backscatter LIDAR for vertical profiling of moisture, aerosol extinction, backscatter, and LIDAR ratio, *Appl. Phys. B*, **55**, 18-28.
- Bond, T. C., Anderson, T. L. and Campbell, D., (1999): Calibration and intercomparison of filter-based measurements of visible light absorption by aerosols, *Aerosol Sci. Technol.*, **30**, 582-600.

- Doherty, S., Anderson, T. L. and Charlson, R. J., (1999): Measurement of the lidar ratio for atmospheric aerosols using a 180°-backscatter nephelometer, *Appl. Optics*, **38**, 1823-1832.
- Ferrare, R. A., Melfi, S. H., Whiteman, D. N., Evans, K. D. and Leifer, R., (1998): Raman lidar measurements of aerosol extinction and backscattering 1. Methods comparison, *J. Geophys. Res.*, **103**, 19663-19672.
- Ferrare, R. A., Turner, D. D., Brasseur, L. H., Feltz, W. F., Dubovik, O. and Tooman, T. P., (2001): Raman lidar measurements of the aerosol extinction-to-backscatter ratio over the Southern Great Plains, *J. Geophys. Res.*, in press.
- Foot, J. S. and Kilsby, C. G., (1989): Absorption of light by aerosol particles: an intercomparison of techniques and spectral observations, *Atmos. Environ.*, **23**, 489-495.
- Karyampudi, V. M., Palm, S. P., Reagan, J. A., Fang, H., Grant, W. B., Hoff, R. M., Moulin, C., Pierce, H. F., Torres, O., Browell, E. V. and Melfi, S. H., (1999): Validation of the Saharan dust plume conceptual model using lidar, Meteosat, and ECMWF data, *Bull. Amer. Met. Soc.*, **80**, 1045-1075.
- Kasten, R., (1969): Visibility in the prephase of condensation, *Tellus*, **21**, 631-635.
- Kent, G. S., Trepte, C. R., Skeens, K. M. and Winker, D. M., (1998): LITE and SAGE II measurements of aerosols in the southern hemisphere upper troposphere, *J. Geophys. Res.*, **103**, 19111-19127.
- Klett, J. D., (1981): Stable analytic inversion solution for processing lidar returns, *Appl. Opt.*, **20**, 211-220.
- Koloutsou-Vakakis, S., Carrico, C. M., Li, Z., Rood, M. J. and Ogren, J. A., (1999): Aerosol properties and radiative forcing at an anthropogenically perturbed mid-latitude Northern Hemisphere continental site, *Phys. Chem. Earth Pt C*, **24**, 541-546.
- Koloutsou-Vakakis, S., Rood, M. J., Nenes, A. and Pilinis, C., (1998): Modeling of aerosol properties related to direct climate forcing, *J. Geophys. Res.*, 17009-17032.
- Masonis, S. J., (2001): An empirical study of the lidar ratio and its variability, with implications for determining climate forcing by satellite-borne lidar. Seattle, WA, University of Washington: 259.
- Masonis, S. J., Franke, K., Ansmann, A., Mueller, D., Althausen, D., Ogren, J. A., Jefferson, A. and Sheridan, P. J., (2000): An intercomparison of aerosol light extinction and 180° backscatter as derived using in-situ instruments and Raman lidar during the INDOEX field campaign, *J. Geophys. Res.*, **in press**,
- Mishchenko, M. I., Lasis, A. A., Carlson, B. E. and Travis, L. D., (1995): Nonsphericity of dust-like tropospheric aerosols: implications for aerosol remote sensing and climate modeling, *Geophys. Res. Lett.*, **22**, 1077-1080.
- Muller, D., Wandinger, U., Althausen, D., Mattis, I. and Ansmann, A., (1998): Retrieval of physical properties from lidar observations of extinction and backscatter at multiple wavelengths, *Appl. Optics*, **37**, 2260-2263.
- Powell, D. M., Reagan, J. A., Rubio, M. A., Erxleben, W. H. and Spinhirne, J. D., (2000): ACE-2 multiple angle micro-pulse lidar observations from Las Galletas, Tenerife, Canary Islands, *Tellus*, **52B**, 652-661.
- Reagan, J. A., Apte, M. V., Ben-David, A. and Herman, B. M., (1988): Assessment of aerosol extinction to backscatter ratio measurements made at 694.3 nm in Tucson, Arizona, *Aerosol Sci. Technol.*, **8**, 215-226.



- Reagan, J. A., Apte, M. V., Bruhns, T. V. and Youngbluth, O., (1984): Lidar and balloon-borne cascade impactor measurements of aerosols: A case study, *Aerosol Sci. Technol.*, **3**, 259-275.
- Rosen, J. M. and Kjome, T., (1997b): Balloon-borne measurements of the aerosol extinction-to-backscatter ratio, *J. Geophys. Res.*, **102**, 11165-11169.
- Rosen, J. M., Pinnick, R. G. and Garvey, D. M., (1997a): Measurement of extinction-to-backscatter ratio for near-surface aerosols, *J. Geophys. Res.*, **102**, 6017-6024.
- Sasano, Y. and Browell, E. V., (1989): Light scattering characteristics of various aerosol types derived from multiple wavelength lidar observations, *Appl. Optics*, **28**, 1670-1679.
- Seinfeld, J. H., Charlson, R. J., Durkee, P. A., Hegg, D., Huebert, B. J., Kiehl, J., McCormick, M. P., Ogren, J. A., Penner, J. E., Ramaswamy, V. and Slinn, W. G. (1996). Aerosol Radiative Forcing and Climate Change, Washington, D. C., National Research Council, National Academy Press.
- Spinhirne, J. D., Reagan, J. A. and Herman, B. M., (1980): Vertical distribution of aerosol extinction cross section and inference of aerosol imaginary index in the troposphere by lidar technique, *J. Appl. Meteo.*, **19**, 426-438.
- Stephens, G. L., Vaughan, M., Engelen, R. J. and Anderson, T. L., (2001): Toward retrieving properties of the tenuous atmosphere using space-based Lidar measurements, *J. Geophys. Res.*, in press as of July, 2001.
- Welton, E. J., Voss, K. J., Gordon, H. R., Maring, H., Smirnov, A., Holben, B., Schmid, B., Livingston, J. M., Russell, P. B., Durkee, P. A., Formenti, P. and Andreae, M. O., (2000): Ground-based lidar measurements of aerosols during ACE-2: instrument description, results, and comparisons with other ground-based and airborne measurements, *Tellus*, **52B**, 636-651.
- Welton, E. J., Voss, K. J., Quinn, P. K., Campbell, J. R., Spinhirne, J. D., Gordon, H. R. and Johnson, J. E., (2001): Measurements of aerosol vertical profiles and optical properties during INDOEX 1999 using micro-pulse lidars, *J. Geophys. Res.*, in press.
- Winker, D. M., Couch, R. H. and McCormick, P., (1996): An overview of LITE: NASA's Lidar In-space Technology Experiment, *Proc. IEEE*, **84**, 164-180.
- Young, S. A., Cutten, D. R., Lynch, M. J. and Davies, J. E., (1993): Lidar-derived variations in the backscatter-to-extinction ratio in Southern Hemisphere coastal maritime aerosols, *Atmos. Environ.*, **27A**, 1541-1551.